DYNAMIC FAILURE AND ENERGY ABSORPTION OF COMPOSITES WITH TOPOLOGICAL CONTROL

Dahsin Liu, Peter J. Schulz
Michigan State University

Keywords: *low-velocity impact, arched composites, energy absorption*

Abstract

The scope of this study was to investigate the relationship between laminated composite curvature and energy absorption for low-velocity impact. All specimens were made of the same prepreg tape material and a cross-ply stacking sequence of $[0/90]_{3s}$ *such that a comparison between flat panels and arched specimens can be made. Analysis of the load-deflection relation, the energy profile and the damage process were of primary interest as they provide the insight into the impact behavior of composites, such as peak load, deflection at the peak load, specimen stiffness, maximum specimen deflection, contact duration, energy absorption and damage modes. The specific energy absorption capability increased with the increase of arch camber.*

1 Introduction

Energy absorption capability is an important indicator of material's tolerance to loading. Materials with high energy absorption capability are usually found to have high resistance to impact and crash loading, and hence are useful for high-performance structures such as aircrafts and ground vehicles. Owing to their high stiffness and high strength with low density, fiber-reinforced composite materials are superior to conventional metals in weight saving. The composite materials also outperform conventional metals in energy absorption as they develop complex damage modes and undergo sophisticated damage process when they are loaded by impact and crash forces.

Flat composite panels can have improved energy absorption capability if their microscopic fiber geometry can be tailored to match with the loading process. For example, composite materials with small fiber angle between adjacent layers and between weaving strands were found to have higher energy absorption capability than conventional cross-ply laminates by 10-20% [1]. Further improvement seems to be promising if innovative fiber microstructure can be formulated. Besides microscopic fiber geometry, global structure geometry can also help to improve energy absorption capability. Arched composites are one of the simplest structure components deviating from flat composites. Their energy absorption capability is of interest in this study.

The arch is a common structural feature, which supports a structure, yet leaves space for access. It is unique in that stresses are distributed in plane. With the topological design of the arch and fiber angles, a unique energy absorbing structure can be designed. Some study has been done on arched laminated composites, but typically for measuring the impact response, characterizing the damage, studying the stress distribution and identifying the buckling process. For example, work done by Kistler and Waas [2] was aimed to characterize the response of arched composite panels due to impact. They showed that, as the thickness decreased, the curvature effects became more important. They concluded that flat panels responded to impacts with larger peak forces but smaller maximum deflections than the arched panels. Kim, Im, and Yang [3] in a similar study mentioned that as the panel became flat, the impact force increased.

Work done by Ambur et al. [4] showed that the arched composites dissipated energy due to structural deformation and retained higher residual stiffness than a flat panel. In another work by Ambur et al [5], the contact force initially increased as the radius of curvature became large. Eventually the contact force decreased as the radius of curvature continued to increase.

Work done by Short, Guild, and Pavier [6] on impact on arched composites showed a linear trend of damage area with increasing impact energy for a flat panel and two different radii. Ging et al [7] showed that low-velocity drop-weight impact tests

in the transverse direction of cylinders with fibers angles at $\pm 55^{\circ}$, there was a nonlinear trend overall in the damage area with increasing impact energy after a certain energy level. The trend initially had a very sharp slope and after approximately 6J of energy the slope decreased dramatically. Work on the energy absorption due to impact and crash loading and the effects of curvature was not widely studied. It will be the primary research in this study.

2 Fabrication of Arched Composites

The fabrication process consisted of layering prepreg tape, molding the tape onto steel arched molds and curing the arched laminates in an autoclaving process. All arched specimens were fabricated from a glass/epoxy prepreg tape. They were twelve plies with a symmetric stacking sequence to avoid any additional warpage due to unsymmetric thermal contraction after curing. Some flat panels were also cured in the autoclave for comparison.

A conventional stacking sequence of $[0/90]_{3s}$ was chosen for this study with 0^{o} fibers aligned in the axial direction and 90^{o} fibers in the transverse direction of the arched mold, resulting in orthotropic arched composites. In manufacturing, the prepreg tape was first cut into 30.48cm x 30.48cm layers. For flat panels, twelve layers of tape were stacked into a laminate. The thickness of the cross-ply laminate was maintained at 0.249cm. For arched specimens, the laminate was further cut into 7.0cm wide strips. The strips were then trimmed to desired lengths such that they could be wrapped onto molds without any excess.

Three arches with different cambers were prepared. They were called small, medium and large arches. Figure 1 shows the dimensions of each arch. The span of each arch was maintained at 7.62cm. The "wings" on either side were maintained at 2.54cm. Hence, the laminated strip length was 12.7cm for the small arch, 13.46cm for the medium arch and 13.97cm for the large arch. Other dimensions of the arches, e.g. camber or arch height (y), radius of curvature (r) and arc length are also listed in Table 1. The arc length does not include the "wing" portions, just the curvature.

3 Testing of Arched Composites

All specimens were tested using a low-velocity instrumented drop-weight impact system [8]. The

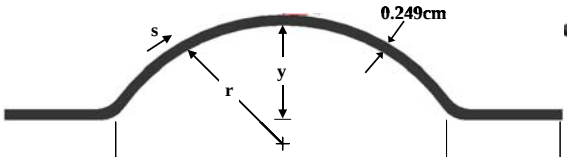

Figure 1 - Schematic of end view of arched composite with dimensions.

Table 1 – Arch and mold dimensions.

Mold Type	Camber (y) cm	Radius of Curvature (r) cm	Arc Length (s) cm
Small	0.80	8.41	7.62
Medium	1.59	5.72	8.38
large	2.07	4.45	8.89

histories of impact load, deflection, velocity, and absorbed energy were obtained subsequently with the use of a computer program based on Newton's second law and mathematical integration. Calculation was also done to determine the impact energy, i.e. the energy introduced to the specimens, so that a comparison could be made with the absorbed energy, i.e. the energy absorbed by the specimens. Each test was run under the same conditions and setup to eliminate additional variables beyond adjusting the impact energy.

The impact system has a crosshead, which consists of a load cell tup and two flags, and is attached to a rail clamp. The load cell has a 22,241N capacity and a 1.27cm hardened steel hemispherical tip for impacting the specimens. Assumed to be perfectly rigid, the load cell measures the load during impact. The two flags run through the infrared detector right before impact to record the impact velocity at the moment of contact between the specimen and tup tip. The contact velocity is obtained by dividing the distance between the flags with the time it takes the flags to run through the detector. The rail clamp allows adjustment of the height of the crosshead on the guide rails. The latch is pressed to release the crosshead from the rail clamp. If the impact energy is low enough, the crosshead/tup will rebound several times, further damaging the specimen. To prevent this, a rebounding system is in place.

During impact testing, specimens were clamped at the base of the testing equipment such that the tup tip impacted the center of the specimens. Three methods for clamping specimens were designed in the study, bar-clamped, frame-clamped and bolted. When the specimens were clamped at each end, i.e. the winged section, independently by a bar, the boundary condition was called bar-clamped. The bar-clamped ends could displace with each other. If the two end bars were joined together by two additional bars to form a frame, the displacement between the winged sections could be reduced significantly. This boundary condition was called frame-clamped boundary condition. However, slippage between the specimens and the frame could still happen. In order to completely eliminate the slippage, additional holes at the two ends of the frame were prepared to bolt the specimens, resulting in bolted boundary condition.

4 Energy Analysis

When impact takes place, the load cell records the tup load, *F(t)*. To find the acceleration, Equation (1) is used, where the tup load is divided by the the total impact mass, *m*. The data is recorded every 25μs.

$$a(t) = F(t)/m. \quad (1)$$

From the acceleration calculation in Equation (1) and the contact velocity, the velocity history of the tup can be determined. Equation (2) is the numerical integration of the acceleration over time. Since the tup is decelerating during the impact, the integration is multiplied by –1. The contact velocity v_i is determined by the infrared detector and is added to this integration.

$$v(t) = -\int_0^t a(t)dt + v_i \quad (2)$$

Equation (3) shows the calculation to determine the deflection of the specimen during impact. The velocity is integrated over time from zero to the final time of the impact.

$$\delta(t) = \int_0^t v(t)dt \quad (3)$$

The data acquisition program also calculates the absorbed energy by integrating the area enveloped by the load-deflection curve.

The load-deflection relation is the most fundamental way to describe behavior of composites during impact. A load-deflection relation can be established by plotting the force against the corresponding displacement throughout the entire impact event. It provides the majority of data for impact analysis. This relation can also give insight to how a composite damages. Most important, it shows how the composite absorbs the impact energy throughout the impact process.

There are two general types of load-deflection curves based on whether or not the tup tip penetrates the specimen or rebounds. Figure 2 shows these two types of curves for a frame-clamped flat panel and a bolted medium arch. For frame-clamped flat panel, the closed curve results from an impact with rebounding while the open curve from an impact with penetration. For the closed curve, notice how the load increases to a peak load and loops back to the start such that the load decreases as the deflection also decreases. This looping back of the curve is due to the crosshead and tup rebounding upwards, which causes the load to decrease as the specimen deflects back.

Penetration takes place as the tip embeds into the specimen. Once penetration is reached, there is no rebounding of crosshead and tup, resulting in an open curve. When the tup tip punches through the specimen, it is defined to be perforation. Once perforation is reached, there is still a small load due to the tup tip rubbing on the specimen. Since the specimen has been perforated, this small load is not considered in the energy absorption calculation.

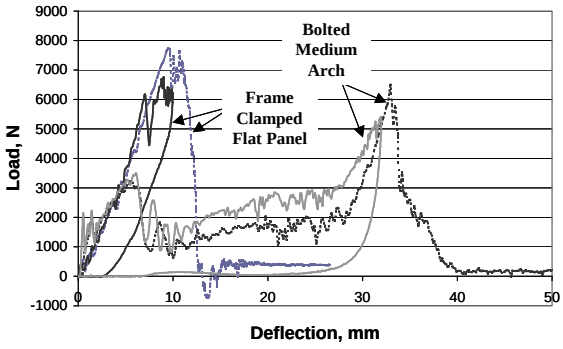

Figure 2 - Load-deflection curves for frame-clamped flat panel and bolted medium arch.

In comparison, the load-deflection relations for bolted medium arch are also shown in Figure 3. The

shape of the curves has changed dramatically. There are two major peaks and a much larger maximum deflection. The maximum load is approximately 6,500N and the maximum deflection around 4cm. There are four closed curves and four open curves.

The energy absorbed by the composite during impact is calculated via Equations (4) and (5). It is simply the determination of the area bounded by the load-deflection curves. The load $f(\delta)$ defined in Equation (4) is integrated over the deflection δ. The upper limit δ_t is taken as the final deflection for closed curves. For the open curves, the limit δ_t is determined by the extension method, which is explained in the next section.

$$F = f(\delta) \tag{4}$$

$$E_a = \int_0^{\delta_t} f(\delta)d\delta \tag{5}$$

Determining the area for integration on the open load-deflection curves is critical for obtaining accurate energy absorption. A line is usually extended to the abscissa at the same slope as the descent of the load during the penetration process. This line is the extension of the load-deflection curve to eliminate the effects of the friction due to the rubbing of the tup with the specimen after perforation. The location where the extension intersects the abscissa is the upper bound, δ_t. This technique can also be applied to closed load-deflection curves which end very close to the end of open curves.

The equations for determining the impact energy are given below in Equations (6) and (7). It consists two components, The first component is the kinetic energy due to kinetic energy right before contact-impact takes place. The variable m is the mass of the crosshead/tup. The initial velocity v_i is contact velocity measured by the infrared sensor/emitter. The second component of the impact energy is the potential energy generated by the deflection h' of the specimen from the contact position to the lowest position. This deflection is also termed as the maximum deflection. It is where the extension line intersects the abscissa for open curves. For closed curves, it is the maximum deflection the specimen ever experiences.

$$E_i = \frac{1}{2}mv_i^2 + mgh' = mgh + mgh' \tag{6}$$

The energy profile is the key to characterizing the energy absorption of the composite. The energy profiles shown in Figure 4 are for a bolted flat panel and bolted medium arch. The impact energy (E_i) is plotted on the abscissa and the absorbed energy (E_a) on the ordinate. The scales for both axes are intentionally the same such that a line can be drawn at a $45°$ angle, which is the equal energy line.

As the impact energy increases, the absorbed energy also increases. Once the impact becomes fairly close to the absorbed energy, i.e. close to the equal energy line, penetration takes place. This close relation will maintain until perforation takes place. After that, the absorbed energy will be more or less constant. In Figure 4, the bolted flat panel has absorbed energy around 47J while the bolted medium arch has 90J.

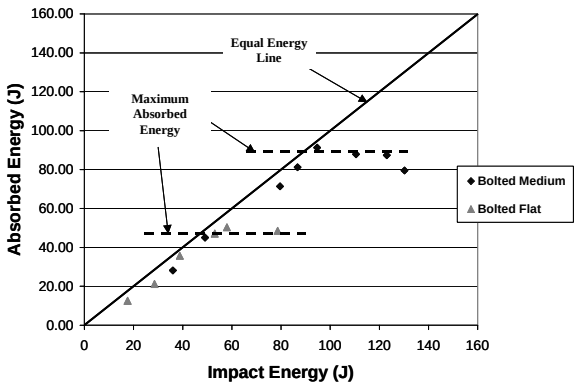

Figure 3 - Energy profiles for bolted flat panel and bolted medium arch specimens.

5 Camber Effect

The effects of the arch camber on the load-deflection relation should provide insight to an even more effective design for energy absorption. For structure applications, a composite component should be able to absorb as much energy as possible while maintaining reasonable integrity after being impacted. With the increase of curvature, a composite specimen has more material aligned along the impact direction, the impact resistance should be increased accordingly. However, the gross mass of the specimen is also increased. An optimal curvature may be identified.

Figure 4 shows a typical load-deflection curve from each of the three types of arch composites with bolted boundary condition as well as a bolted flat panel. The flat panel is 69.85mm wide like the

arches and is 127mm long so that only 25.4mm on each end is bolted like the arches.

Several important features should be noted. There are two maximum loads in the arched composites; the first, i.e. the initial maximum load, occurs about 6mm of deflection and the second, i.e. the peak load, is located at different deflection value depending on the arch size. The flat panel has no initial maximum load and its stiffness is similar to those of the arches. For the arched composites, the region between the two maximum loads looks like a saddle shape and tends to increase as the curvature of the composite increases. The flat panel has zero curvature and there is only one peak load and no saddle region.

Measuring the two maximum loads and associated deflections and plotting their relation will help to sort out the curvature effects. Figure 4 shows a plot for the first peak load and the corresponding deflections for the three arch sizes. The load measurements are taken from individual tests. The diamonds are the data points for the small arches, which have the lowest initial maximum force, followed by the medium arch, and the large arch has the highest initial maximum force. It can be concluded from this diagram that the initial maximum load increases as the curvature increases. This result is likely due to the fact that more material is aligned along the impact direction when the curvature increases.

The results for the second peak load and corresponding deflections can be seen below in Figure 7.1.3. The general trend is that the peak load decreases as the curvature increases, while the corresponding deflection increases. The increase in the deflection is due to the height of the arch, which allows the composite to deflect more before being perforated. The decrease in the peak load may be due to the fibers not being as stiff because they are not pulled as taunt as a flat panel or small arch.

The energy profile provides some details of the energy absorption process. Table 2 summarizes the absorbed energy for the flat panel, small, medium, and large arches with bolted boundary condition. There is a clear trend that as the curvature increases the maximum energy absorption increases.

It also shows the mass and the ratio of absorbed energy to mass. The ratio gives an indicator of the trade-off of weight to energy absorption. The data shows that the weight increases with increasing curvature. The absorbed energy of the flat panel is

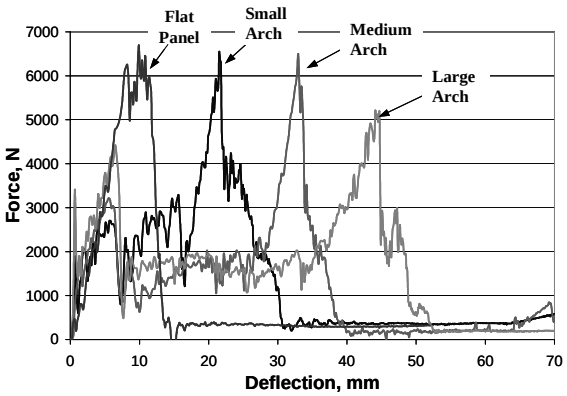

Figure 4 - Typical load-deflection curves for bolted arches and flat panel.

Table 2 - Bolted specimens mass and maximum absorbed energy.

	Mass (g)	Max. Absorbed Energy (J)	Max. AE/Mass (J/g)
Flat Panel	42.2	50	1.19
Small	43.1	83	1.93
Medium	44.6	91	2.04
Large	47.6	108	2.27

about 71 Joules, the small arch 83 Joules, the medium arch 91 Joules, and the large arch 108 Joules. Looking at the ratio of the maximum absorbed energy (AE) to the mass, it can be seen that the large arch has the best energy absorption to mass ratio.

6 Damage Process

Fiber breakage and delamination traveled the top of each specimen in the transverse (90°-direction) direction. The fiber breakage was visible at the initial stages of damage, where it began at the free edges and propagated towards the center. The fiber breakage began at the top surface and worsened as the delamination became more pronounced. Figure 5 shows an oblique side view of a damaged composite. The delamination and fiber breakage near the top surface can be easily seen. Notice how the top layers are completely fractured along the width of the specimen.

Figure 6 shows a top view of the specimen in Figure 5. Faint changes in the shades of the color show the delamination patterns on the top of the specimen. The fiber breakage along the

transverse direction can be seen. The side view shows more of the extensive damage.

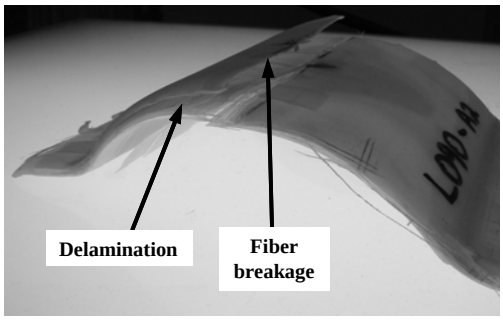

Figure 5 - Side view of damaged bolted $[0/90]_{3s}$ large arch composite.

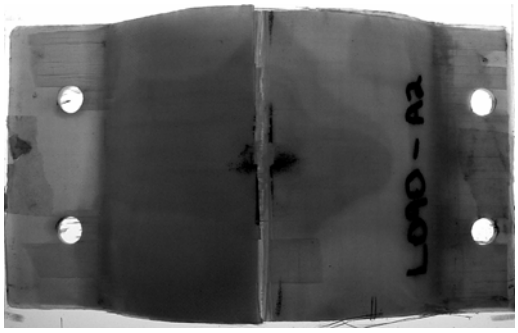

Figure 6 - Top view of damaged bolted $[0/90]_{3s}$ large arch composite.

A top view of a damaged frame clamped specimen can be seen in Figure 7. It is on a light table, which shows the delamination patterns. The delamination is in oval patterns with the major axes along the axial direction (0°-direction). If the impact energy is great enough, the delamination will spread to the clamped wings. There is also rectangular shaped delamination at the center of the arch, which extends to the edges at an oblique angle to the axis of the arch. This rectangular delamination is able to take place due to the extensive fiber breakage. Notice the rectangular shaped delamination area near the transition from the arch to the winged sections. This delamination takes place due to the bending of the sides. For the bolted specimens, the delamination near the top center and from the bending of the sides meets causing complete delamination of the layers. As the specimen buckles the damage progressively increased by delamination and fiber breakage in the layers at the peak of the arch.

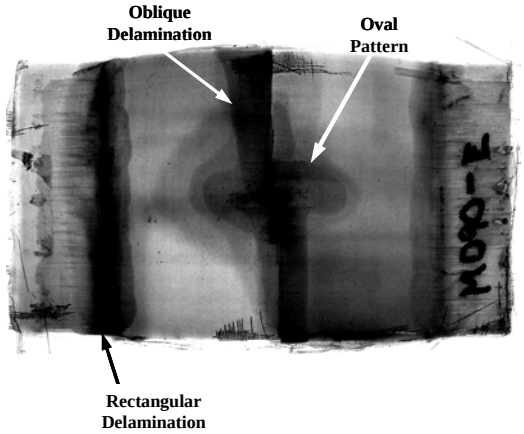

Figure 7 - Top view of delamination of $[0/90]_{3s}$ frame clamped medium arch showing delamination pattern.

7 Buckling Process

The buckling process is a very complex phenomenon, which can be roughly represented by the schematic shown in Figures 8. The figure shows a single load-deflection curve that is representative of a damaged specimen. The energy-deflection relation is also plotted. The curve is marked by six critical points in the process, lettered A through F. Next to each load-deflection curve is a scaled schematic showing the buckling and bending of the specimen during the impact process. The schematic begins with the initially undamaged specimen, followed by the damaged specimen at deflection points B-F, where the deflection of the center of the specimen is the only known point. The deformed profiles were created with resemblance to quasi-static loading results. Initially, each specimen is in its original undamaged state point A. Then the composite is impacted and the load rises to point B. The load then drops from point B to point C with very little deflection. The critical buckling load or onset of buckling is at point B. The specimen then deflects to the point where it ends up in an inverted state, which occurs at point D. The peak of this load is at point E where the specimen is either in a completely inverted state (twice the original height of the arch) or in a hyper-inverted (more than twice the original height of the arch). At point F, all specimens will be in a hyper-inverted state because

enough delamination and fiber breakage has taken place allowing the specimen to deflection beyond twice the original height of the arch.

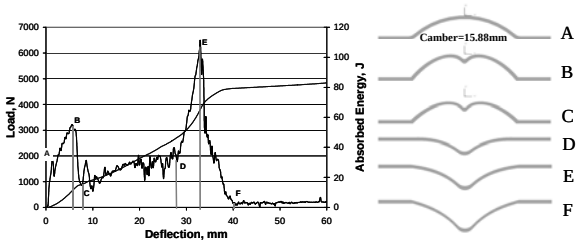

Figure 8 - (a) Common bolted medium arch load-deflection curve (b) Schematic of specimen buckling and deflection at critical points.

8 Summary

In order to understand how the energy is absorbed, the buckling and damage process must be studied. Buckling typically increases the complexity and instability of the damage process creating less predictability and difficulty in characterizing the damage. If buckling is reduced, more control over the specimen damage process will allow precise damage control, which in turn will allow control in energy absorption. In this study, it was believed that buckling occurred more apparently in the specimens with the bolted boundary condition due to the specimen being unable to slip. Frame clamping would allow the specimen to smoothly bend during impact. The slippage of the specimen at the clamping boundaries allowed the specimen to bend and deflect downward, without large drops in load, which are associated with buckling. By bolting the specimen, the boundaries were fixed, forcing the specimen to suddenly fail, which is apparent by sudden load drops. The peak load before this sudden load drop is the onset of buckling. Bolting the specimen increased the visible delamination and fiber breakage and several times the specimen actually broke into two pieces because of the high impact energy.

References

[1] Liu, D., "Characterization of Impact Properties and Damage Process of Glass/Epoxy Composite Laminates" J. Composite Materials, 38(16), 1425-1442, 2004.

[2] Kistler, L.S., Waas, Anthony M., "On the response of curved laminated panels subjected to transverse impact loads," *International Journal of Solids and Structures*, Vol 36, 1999, pp. 1311-1327.

[3] Kim, Y-N, Im, K-H, and Yang, I-Y, "Characterization of Impact Damages and Responses in CFRP Composite Shells," *Materials Science Forum*, Vols. 465-466, 2004, pp. 347-252.

[4] Ambur, D.R., Starnes, H. Jr., "Effect of curvature on the impact damage characteristics and residual strength of composite plates," *39th AIAA/ASME/ASCHE/AHS/ASC Structures, Structural Dynamics, and Materials Conference*, AIAA Paper No. 98-1881, 1998.

[5] Ambur, D.R., Chunchu, P.B., Rose, C.A., Feraboli, P., Jackson, W.C., "Scaling the non-linear impact response of flat and curved anisotropic composite panels," *46th AIAA/ASME/ASCE/AHS/ASC Structures, Dynamics and Materials Conference*, No. 2005-2224, Austin, TX, 2005.

[6] Short, G.J., Guild, F.J., Pavier, M.J., "Post-impact compressive strength of curved GFRP laminates," *Composites Part A: applied science and manufacturing*, Vol. 33, 2002, pp. 1487-1495.

[7] Gning, P.B., Tarfaoui, M., Collombet, F., Davies, P., "Prediction of damage in composite cylinders after impact," *Journal of Composite Materials*, Vol. 39, No. 10, 2005, pp. 917-928.

[8] Coppens, G.J., Effects of Three-dimensional Geometry on Penetration and Perforation Resistance, M.S. Thesis, Michigan State University, May, 2004.